

Kinetic Investigations of Bridge Formation and Cleavage in Hydroxo-Bridged Chromium(III) Dimers with Facially Coordinated Ammonia

Peter Andersen* and Anders Døssing

Department of Chemistry, H. C. Ørsted Institute, University of Copenhagen, Universitetsparken 5, DK-2100 Copenhagen Ø, Denmark

Andersen, P. and Døssing, A., 1993. Kinetic Investigations of Bridge Formation and Cleavage in Hydroxo-Bridged Chromium(III) Dimers with Facially Coordinated Ammonia. – Acta Chem. Scand. 47: 1–8.

The monohydroxo-bridged chromium(III) dimer $[(\text{H}_2\text{O})_2(\text{NH}_3)_3\text{Cr}(\text{OH})\text{Cr}(\text{NH}_3)_3(\text{H}_2\text{O})_2]^{5+}$ (with NH_3 facially coordinated) and its deprotonated forms establish equilibrium with the *cis*- and *trans*-isomers of the dihydroxo-bridged species, $[(\text{H}_2\text{O})(\text{NH}_3)_3\text{Cr}(\text{OH})_2\text{Cr}(\text{NH}_3)_3(\text{H}_2\text{O})]^{4+}$, with half-lives from 2 to 34 min at 25.0°C in 1.0 M $(\text{Na,H})\text{ClO}_4$ in the $[\text{H}^+]$ range 10^{-7} –1 M. The kinetics of this bridge formation and cleavage was studied spectrophotometrically under these conditions.

From the kinetic data it was possible to determine the rate constants for the conversion between the 4+ and 3+ charged species, respectively, and the rates of an acid-catalyzed pathway through a 5+ charged aquahydroxo-bridged intermediate. A bridge formation/cleavage mechanism, related to, but different from that involved in the *cis*–*trans* isomerization, is proposed. The observed enhanced rates in these processes are explained by the presence of intramolecular hydrogen bonds between oxygen atoms at the two metal centers during the course of reaction.

From these kinetic experiments, in combination with previous acid–base titrations and equilibrium measurements, the acid dissociation constants and the equilibrium ratios of the involved species were also determined. The relatively high stability of some of these hydroxo-bridged dimers is likewise explained by intramolecular hydrogen bonds, $\text{Cr}(\mu\text{-H}_3\text{O}_2)\text{Cr}$ being the dominant type.

In a recent publication¹ we dealt with the kinetics of the *cis*–*trans* isomerization of chromium(III) dimers of the type $[(\text{H}_2\text{O})\text{L}_3\text{Cr}(\text{OH})_2\text{CrL}_3(\text{H}_2\text{O})]^{4+}$ and deprotonated forms, where L_3 was facially coordinated $(\text{NH}_3)_3$ or 1,4,7-triazacyclononane (tacn), *cis* and *trans* referring to the positions of the water and non-bridging hydroxide ligands relative to the $\text{Cr}(\text{OH})_2\text{Cr}$ bridge plane. The kinetic experimental data were explained by an isomerization model with a direct pathway between the equally charged dihydroxo-bridged dimeric isomers, and it was claimed that within the experimental uncertainty the values of the rate constants obtained were not influenced by a path via monohydroxo-bridged species. The argument for this was based on parts of the present work, which deals in more detail with the kinetic behaviour of the condensation of the monohydroxo-bridged dimers to the dihydroxo-bridged ones and the reverse bridge cleavage process, L_3 being *fac*– $(\text{NH}_3)_3$.

A limitation to these studies has been the disturbing loss of ammonia most pronounced at $[\text{H}^+] < 10^{-5}$ M. However, this disadvantage is outweighed by the fact that

the mono-, di- and trihydroxo-bridged dimers with L_3 being *fac*– $(\text{NH}_3)_3$ are all available in well defined salts. It has not yet been possible to detect the mono- and trihydroxo-bridged tacn dimers. On the other hand, the robustness of the dihydroxo-bridged tacn dimer was an advantage in the study of the *cis*–*trans* isomerization, and in this way the $(\text{NH}_3)_3$ and tacn systems have complemented each other.

Results

As the following will show, some simplifications have been used in the experiments as well as in the calculations in order to handle the complicated system of reversible reactions between the monohydroxo-bridged and the *cis*- and *trans*-isomers of the dihydroxo-bridged dimers with various charges. Comparison between constants determined in this work and by other methods^{1,2} shows good agreement, and further justification for the simplifications used is given in the following sections.

The conversion between mono- and dihydroxo-bridged dimers. The reaction scheme for the conversion between the mono- and dihydroxo-bridged dimers is given in

* To whom correspondence should be addressed.

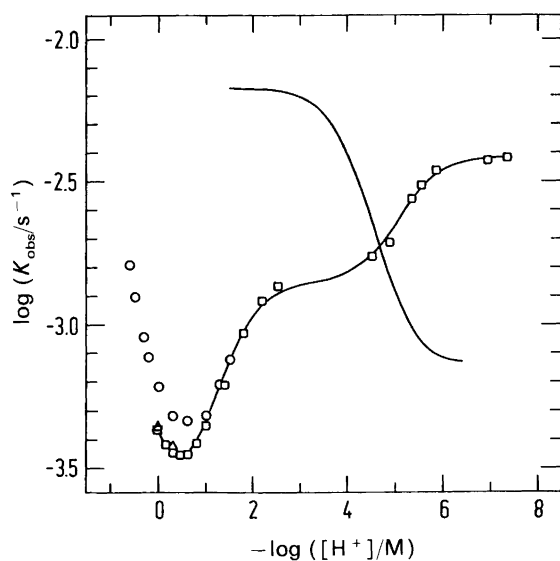
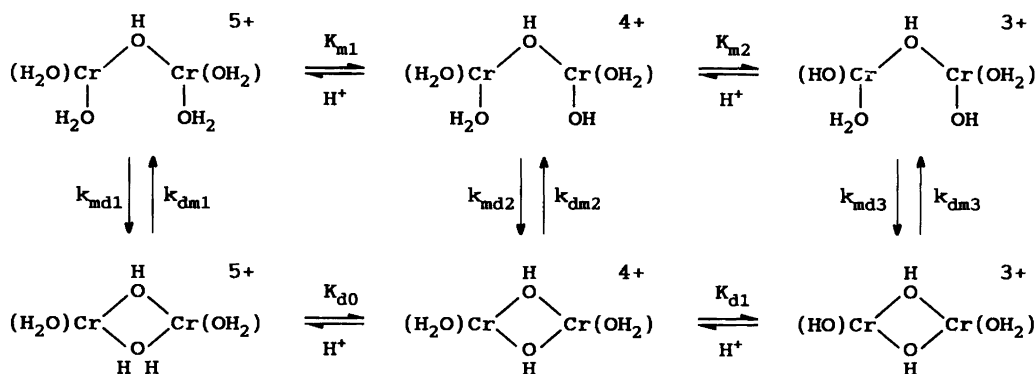


Fig. 1. $\log(k_{\text{obs}}/\text{s}^{-1})$ vs. $-\log([\text{H}^+]/\text{M})$ for the bridge formation/cleavage in experiments in which the absorbance of the dihydroxo-bridged *cis*-isomer equals that of the *trans*-isomer. (\square) represents experiments starting with monohydroxo-bridged dimer and (Δ) those starting with the dihydroxo-bridged *trans*-isomer [25.0°C, 1.0 M (Na,H)ClO₄]. (\circ) represents experiments in 4.0 M (Li,H)ClO₄ not included in the calculations. The curve through (Δ) and (\square) is based on eqn. (1) using the constants from Table 1. For comparison the curve for the *cis-trans* isomerization¹ is given as well.

Scheme 1. In this scheme the *cis-trans* isomerization of the dihydroxo-bridged dimers is omitted, and species with charges lower than 3+ are not included. The reactions were primarily followed spectrophotometrically at fixed $[\text{H}^+]$ at wavelengths where the molar absorptivity of the dihydroxo-bridged *cis*-isomer equals that of the *trans*-isomer. Under these circumstances first-order kinetics is observed, and the expression for the pseudo-first-order rate constant as a function of $[\text{H}^+]$ (see Experimental) is given by eqn. (1), where the negligible term, $[\text{H}^+]^2 K_{\text{d}0}^{-1}$



Scheme 1. Reaction scheme for the bridge formation/cleavage showing the symbols used for the rate and equilibrium constants. m = monohydroxo-bridged dimer and d = dihydroxo-bridged dimer (*cis* + *trans*). $k_{\text{dm}2}/k_{\text{md}2} = K_1$.

$$\begin{aligned}
 k_{\text{calc}} = & (k_{\text{md}1}[\text{H}^+]^2 + k_{\text{md}2}K_{\text{m}1}[\text{H}^+] + k_{\text{md}3}K_{\text{m}1}K_{\text{m}2}) \\
 & \times \{([\text{H}^+]^2 + K_{\text{m}1}[\text{H}^+] + K_{\text{m}1}K_{\text{m}2})^{-1} \\
 & + ([\text{H}^+]^2 K_{\text{d}0}^{-1} + [\text{H}^+] + K_{\text{d}1})^{-1} K_1 K_{\text{m}1}^{-1}\} \quad (1)
 \end{aligned}$$

($\ll [\text{H}^+]$), was omitted in the refinements.

The $[\text{H}^+]$ dependence of the observed first-order rate constant is given in Fig. 1. The reactions were initiated with the monohydroxo-bridged dimer, except for a few with $[\text{H}^+]$ between 0.1 and 1 M, where the final equilibrium content of this dimer is sufficiently high to allow a determination of the rate constant, k_{obs} , when also starting with the dihydroxo-bridged *trans*-isomer. The equilibrium ratio between the mono- and dihydroxo-bridged dimers (*cis* + *trans*) is 0.02–0.03 at $[\text{H}^+] < 0.01$ M, and at higher $[\text{H}^+]$ the content of the monohydroxo-bridged dimer increases to nearly 100% with the formation of the 5+ charged ion.² Measurements at $[\text{H}^+] < 10^{-7}$ M were unreliable owing to the loss of ammonia. Fig. 1 includes measurements in 4.0 M (Li,H)ClO₄ with $0.03 < [\text{H}^+] < 4.0$ M, and for comparison the rate constant for the *cis-trans* isomerization of the dihydroxo-bridged dimer is also depicted.¹

Table 1 contains the result of the least-squares refinement using the k_{obs} vs. $[\text{H}^+]$ data on eqn. (1) (see Experimental). Included in the table are the constants used in the refinement and other relevant constants.

In order to distinguish between the rates of condensation from the monohydroxo-bridged to the dihydroxo-bridged *cis*-isomer and to the *trans*-isomer, respectively, a few experiments starting with the monohydroxo-bridged dimer were performed at wavelengths at which the molar absorptivities of these three species differ. The $[\text{H}^+]$ range investigated was $10^{-6} < [\text{H}^+] < 10^{-4}$ M, i.e. around $K_{\text{m}2}$ and $K_{\text{d}1}$, where the equilibrium concentration of monohydroxo-bridged species is only 2% relative to dihydroxo-bridged species.

Using Scheme 2, which implies the simplification that no back-reaction (bridge cleavage) takes place, the biexponential expression for the absorbance (A) vs. time (t), including a linear correction (see Experimental), is

Table 1. Rate constants and equilibrium constants for the conversion between the mono- and the dihydroxo-bridged chromium(III) dimers (Scheme 1) at 25.0°C in 1.0 M (Na,H)ClO₄ as obtained from kinetic measurements combined with results from earlier acid-base titrations and equilibrium experiments^{1,2} (see Experimental). The constants available for the tetraammine- and aquachromium(III) system are also given.

System:	Triammine (this work)	Tetraammine ³	Aqua ^{13,14}
$k_{md1}/10^{-4} \text{ s}^{-1}$	1.6(2)	0.027(3)	0.88(6)
$k_{md2}/10^{-4} \text{ s}^{-1}$	13.7(6)	3.80(4)	4.26(8)
$k_{md3}/10^{-4} \text{ s}^{-1}$	37.6(6)		114(4)
$k_{dm1}K_{d0}^{-1}/10^{-4} \text{ M}^{-1} \text{ s}^{-1}$	2.0 ^a	0.49(5)	0.48(4)
$k_{dm2}/10^{-4} \text{ s}^{-1}$	0.4 ^b	1.21(2)	0.27(3)
$k_{dm3}/10^{-4} \text{ s}^{-1}$	0.7 ^b		
K_1	0.031(4) ^c	0.32(1)	0.063(8)
K_2	0.019 ^d		
K_3	0.028 ^d		
$-\log(K_{m1}/M)$	1.61(8)	1.75	0.96(4)
$-\log(K_{m2}/M)$	5.32(4)		4.30(2)
$-\log(K_{m3}/M)$	8.18(6) ^e		
$-\log(K_{d1}/M)$	5.11 ^f		3.67(1)
$-\log(K_{d2}/M)$	8.35 ^f		5.83(2)
$-\log(K_{t1}/M)$	0.10 ^e		

^a Derived from $k_{dm1}K_{d0}^{-1} = k_{md1}K_{t1}^{-1}$, where $K_{t1} (=K_{m1}K_1^{-1}) = [H^+][d^{4+}]/[m^{5+}]$ (Scheme 1). ^b Derived from $k_{dmn} = K_{n-1}k_{mdn}$ ($n = 2, 3$). ^c Derived from $K_1 = K_{m1}K_{t1}^{-1}$. ^d Derived from $K_{n+1} = K_nK_{m(n+1)}K_{dn}^{-1}$ ($n = 1, 2$). ^e From Ref. 2 (K_{t1} is defined in note a). ^f From Ref. 1 (*cis + trans*).

given by eqn. (2), and the expression for k_{mc} (see Experimental) is given by eqn. (3). In the least-squares

$$A(t)_{\text{obs}} = (A_0 - A_\infty)e^{-k_{md}t} + A_1(e^{-k_d t} - e^{-k_{md}t}) + A_\infty + \alpha t \quad (2)$$

$$k_{mc} = \{k_{md}(A_1 + A_\infty - [m]_0 \epsilon_t) - k_d A_1\} / \{[m]_0(\epsilon_c - \epsilon_t)\} \quad (3)$$

refinement of the absorbance vs. time data to eqn. (2) A_1 , k_{md} and k_d were strongly correlated. In order to get a good determination of A_1 the previously independently determined values of k_{md} and k_d at the actual $[H^+]$ were therefore inserted as constants in the refinements (see Experimental). Values of k_{mc} with an e.s.d. of 5–10% were obtained by inserting in eqn. (3) these rates and the absorbances $[m]_0 \epsilon_c$ and $[m]_0 \epsilon_t$ from separate experiments, and A_∞ and A_1 from the eqn. (2) refinement.

The expression for k_{mc} as a function of $[H^+]$ in the range $10^{-6} < [H^+] < 10^{-4} \text{ M}$, using Scheme 2b, is given by eqn. (4). Least-squares refinement of the k_{mc} vs. $[H^+]$

$$k_{mc} = (k_{mc2}[H^+] + k_{mc3}K_{m2}) / ([H^+] + K_{m2}) \quad (4)$$

data (Fig. 2) to this expression with the K_{m2} value from Table 1 resulted in the k_{mc2} and k_{mc3} rate constants given in Scheme 3. In this scheme $k_{mt2} = k_{md2} - k_{mc2}$ and $k_{mt3} = k_{md3} - k_{mc3}$, and the values of k_{tc1} , k_{ct1} , k_{tc2} and k_{ct2} are those obtained by direct measurements of the isomerization.¹

From the bridge formation rate constants and the known equilibrium ratios between the mono- and the dihydroxo-bridged species (Table 1 and Ref. 2) it is possible to calculate the bridge cleavage rate constants

given in square brackets in Scheme 3. The small magnitude of these constants compared to the bridge formation rate constants (the same order of magnitude as the e.s.d. on the formation rate constants) justifies the above-mentioned simplification in disregarding bridge cleavage in the calculation of the bridge formation constants. Furthermore, it can be seen from Scheme 3 that, as k_{ct1}/k_{cm2} and k_{tc2}/k_{tm3} are well above unity (k_{cm2} and k_{tm3} are the reverse constants of k_{mc2} and k_{m3} , respectively), the values for the isomerization rate constants obtained earlier¹ are not, within experimental error, affected by a pathway via monohydroxo-bridged species. In accordance with this, the biexponential absorbance vs. time

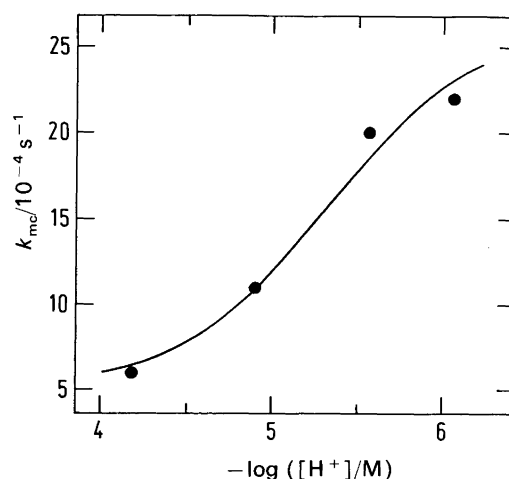
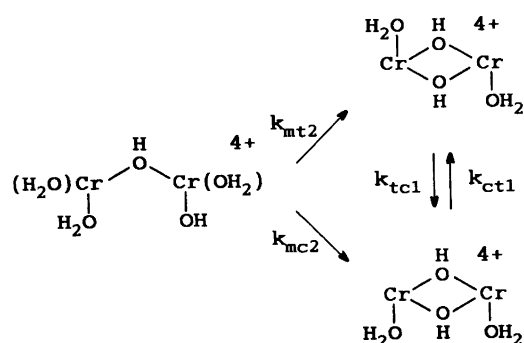
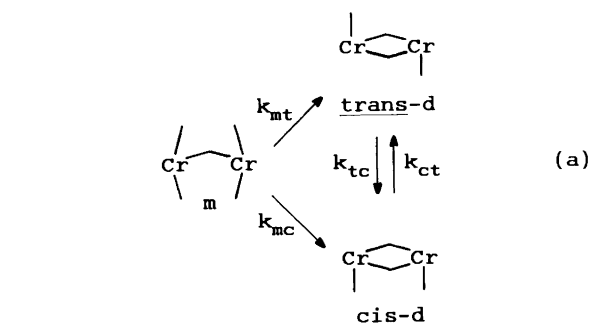
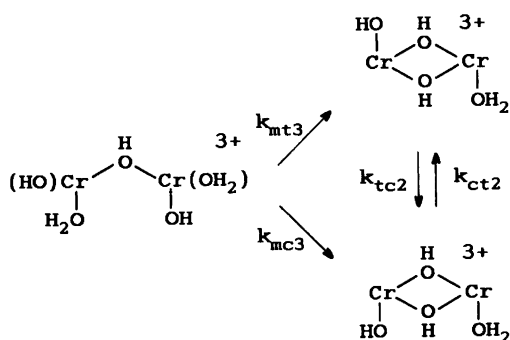


Fig. 2. k_{mc}/s^{-1} vs. $-\log([H^+]/M)$. The experimental k_{mc} points are obtained by use of eqns. (2) and (3), and the curve is based on eqn. (4) using the constants from Table 1 and Scheme 3.



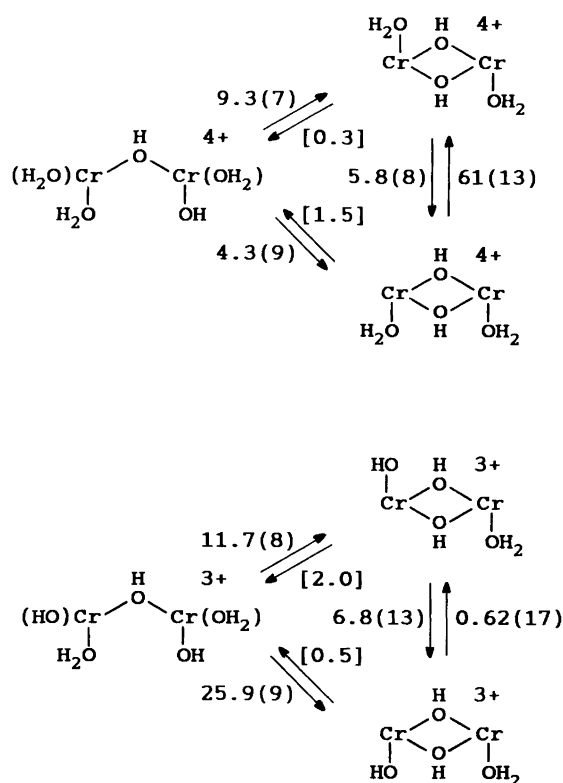
(b)



Scheme 2. Reaction scheme for the bridge formation showing the symbols used for the rate constants. m = monohydroxo-bridged dimer, d = dihydroxo-bridged dimer, c refers to the dihydroxo-bridged *cis*-isomer and t to the *trans*-isomer. $k_{md} = k_{mt} + k_{mc}$ and $k_d = k_{tc} + k_{ct}$.

curves could be separated into two rate constants matching with k_d and k_{md} determined from the separate uni-exponential experiments (see Experimental).

The magnitudes of the rate constants and equilibrium constants have the following consequences for the course of reaction when starting with the monohydroxo-bridged species: At ca. pH 5.5 bridge formation occurs, so that the *cis*- and the *trans*-isomers are produced at a rate ratio equal to their equilibrium ratio. Above pH 5.5 the *trans*-isomer is produced faster than corresponding to this ratio, and a slower *trans* → *cis* isomerization could also be observed, and vice versa below pH 5.5 (see the example



Scheme 3. Reaction scheme showing the calculated rate constants ($/10^{-4} \text{ s}^{-1}$) at 25.0°C in 1.0 M NaClO_4 for the reactions given in Scheme 2b.

in Fig. 4). Below pH 4.7 the *cis*–*trans* isomerization is faster than the bridge formation. At high $[\text{H}^+]$ ($[\text{H}^+] \approx 0.5\text{--}1.0 \text{ M}$), where bridge cleavage could be observed as well as bridge formation, starting with the dihydroxo-bridged *cis*-isomer gave a biexponential absorbance vs. time curve, with the two rate constants also in this case equal to the separately uniexponentially determined k_{md} and k_d . At this high $[\text{H}^+]$ the *cis*–*trans* isomerization is ca. 20 times faster than the bridge cleavage/formation, the *cis*–*trans* equilibrium ratio is 0.095, and the equilibrium ratio between mono- and dihydroxo-bridged species is ca. 1.

Discussion

In the following discussion of the relative stabilities of the hydroxo-bridged dimers and of the rates of bridge formation and cleavage it should be remembered that these subjects have been reviewed only recently in comparison with other metals, mainly cobalt(III), rhodium(III) and iridium(III), and other ligands.³ For this reason the emphasis in the following is on the present triammine system, with comparisons limited primarily to other ammineaquachromium(III) systems.

The relative stabilities of the hydroxo-bridged dimers. In a recent paper¹ we discussed the stabilities of the *cis*-

relative to the *trans*-isomers of the dihydroxo-bridged dimers with equal charge [4+, 3+ or 2+, with L_3 being $(\text{NH}_3)_3$ or *tacn*] in terms of intramolecular hydrogen bonds. The extent of hydrogen bonding in the *cis*-isomer was estimated with the assumption that *cis*-isomers without such bonds have approximately the same acid dissociation constants as the *trans*-isomers where intramolecular hydrogen bonding is negligible. This assumption means that the ratios $K_{cis/trans} = [\text{cis-d}^{n+}] / [\text{trans-d}^{n+}]$ is independent of n when *cis*- d_0 is a dihydroxo-bridged *cis*-dimer with negligible intramolecular bonding. For the $(\text{NH}_3)_3$ system $K_{cis/trans} = 0.095$, and the deviations from this ratio were explained for the 3+ charged ions by a hydrogen-bond stabilization $K_H = 10^{2.1}$ and for the 2+ charged ions by an expectedly much weaker $K'_H = 10^{0.3}$.

In a similar way it is possible to estimate the degree of intramolecular hydrogen bonding in the monohydroxo-bridged dimers with $L_3 = (\text{NH}_3)_3$ if it is assumed that the acid dissociation constants for these dimers without such hydrogen bonds have the following values: K_{m1}^0 close to that of the erythro ion,* *cis*- $[(\text{H}_2\text{O})(\text{NH}_3)_4\text{Cr}(\text{OH})\text{Cr}(\text{NH}_3)_5]^{5+}$, and K_{m2}^0 and K_{m3}^0 close to those of *trans*- $[(\text{H}_2\text{O})(\text{NH}_3)_3\text{Cr}(\text{OH})_2\text{Cr}(\text{NH}_3)_3(\text{H}_2\text{O})]^{4+}$. The result is that $\log K_{H1} = 1.9$, $\log K_{H2} = 2.7$ and $\log K_{H3} = 2.0$, where K_{Hn} ($n = 1-3$) is the concentration ratio between the forms with and without hydrogen bonds for the 4+, 3+ and 2+ charged species, respectively [eqn. (5)].

$$\log (K_{Hn} + 1) = \sum_1^n \log (K_{mn}/K_{m1}^0) \quad n = 1-3 \quad (5)$$

The assumption used means that the ratio $[m_0^{z+}] / [\text{trans-d}^{z+}] = 0.00044$ is independent of z ($z = 2-4$) when m_0^{z+} is a monohydroxo-bridged dimer with negligible intramolecular hydrogen bonding. Owing to the approximate character of the K_H values these have not been statistically corrected, as this will have only a minor effect on their relative magnitudes. K_{m1}^0 should, from statistical reasons, be increased by a factor four compared to the erythro value because of the three extra water ligands. On the other hand, there is a tendency towards a small, probably solvent-related, decrease in the acidity of ammineaqua complexes when the number of water ligands increases at the expense of ammonia ligands,⁴ so that the total increase in acidity is less than that expected solely from statistical reasons.

The magnitudes of K_{H1} and K_{H3} are in good accordance with that of K_H for the 3+ charged dihydroxo-bridged *cis*-dimer, and give strong evidence for the formation of one intramolecular $\text{H}-\text{O} \cdots \text{H} \cdots \text{O}-\text{H}$ hydrogen bond in the 4+ and 2+ charged monohydroxo-bridged species. This is what would be expected, and has been verified⁵ in a salt of $[(\text{H}_2\text{O})(\text{en})_2\text{Ir}(\text{OH})\text{Ir}(\text{en})_2(\text{OH})]^{4+}$

* This acid dissociation constant was earlier determined as $10^{-3.5}$ M in 1 M NaNO_3 at 25°C by one of the authors (P.A.) from a titration curve in which the points were obtained by time-extrapolated pH measurements.

(*en* = 1,2-ethanediamine), in which the intramolecular distance between the non-bridging oxygen atoms is 2.429(9) Å. In the 3+ charged species the formation of two such bonds is possible, and the magnitude of K_{H2} indicates that more than one are present.

The ratios K_1 , K_2 and K_3 between the mono- and dihydroxo-bridged (*cis* + *trans*) dimers with 4+, 3+ and 2+ charge, respectively, are given in Table 1. The value of $K_1 = 0.031$ for the triammine system may be compared to the corresponding value for the tetraammine system where $K_1 = 0.32$. For the triammine system K_1 is composed of $K_1(\text{trans}) = 0.034$ and $K_1(\text{cis}) = 0.36$ [$K_1^{-1} = K_1(\text{trans})^{-1} + K_1(\text{cis})^{-1}$] with a destabilization of the *cis*- relative to the *trans*-isomer of the dihydroxo-bridged species. The reason for this destabilization, also present in the tetraammine case, is not obvious, but the proximity of the two ammonia ligands on the same side of the $\text{Cr}(\text{OH})_2\text{Cr}$ plane (without the possibility for the formation of an intramolecular bridging hydrogen bond) may be part of the explanation. A similar steric explanation has been given for the apparently low stability of other dihydroxo-bridged dimers with bulky amine ligands, where the effect can be so pronounced that the dimer has not been observed.^{6,7} According to this argument the aqua system should have a relatively small K_1 value, which is also the case, as the value here is 0.06 (Table 1).

The rates of bridge formation (/cleavage). At high $[\text{H}^+]$ the conversion between the mono- and the dihydroxo-bridged dimers is accelerated by hydrogen ions, as can be seen from Fig. 1. The enhanced rate can be explained by the formation of increasing amounts of the strong acid $[(\text{H}_2\text{O})(\text{NH}_3)_3\text{Cr}(\text{OH})(\text{H}_2\text{O})\text{Cr}(\text{NH}_3)_3(\text{H}_2\text{O})]^{5+}$, where the aqua bridge functions as the strong acid.³ As it has not been possible to see any spectral signs of this ion even in concentrated strong acid, it is concluded that it has $K_{d0} > 10$ (and consequently $k_{dm1} > 0.002 \text{ s}^{-1}$). Nevertheless the acid-catalyzed pathway contributes 50% at $[\text{H}^+] \approx 0.1 \text{ M}$, the ratio between this pathway and the uncatalyzed one being expressed as $[\text{H}^+]k_{dm1} / (K_{d0}k_{dm2}) = [\text{H}^+]k_{md1} / (K_{m1}k_{md2}) = 4.8[\text{H}^+]$. For the aqua system it is a little smaller ($1.9[\text{H}^+]$), whereas this ratio for the tetraammine system is ca. 10 times smaller ($0.39[\text{H}^+]$), the most striking difference lying in k_{md1} , which for this system is ca. 50 times smaller than for the two other systems (see later and Table 1). The influence of $[\text{H}^+]$ was also investigated in 4 M $(\text{Li,H})\text{ClO}_4$ at high $[\text{H}^+]$, and a similar picture was obtained except that the effect was more pronounced at $[\text{H}^+] > 0.1 \text{ M}$ (Fig. 1). This is in accordance with an expected decrease of the acid dissociation constant [particularly of the highly charged (5+) species] as the ionic strength, I , increases [$-\log K_a$ for the erythro ion at 25°C has been determined as 2.8 at $I = 0.14 \text{ M}$,⁸ as against 3.5 at $I = 1.0 \text{ M}$ (see the previous section)].

Since the stability ratios between the mono- and the dihydroxo-bridged species have been treated in the previous section, the following discussion of the rate

constants will focus on one side only, namely bridge formation, i.e. the k_{md} rate constants. These are composite constants, as the dihydroxo-bridged dimers exist as two isomers, and for the 4+ and 3+ charged ions it has been possible to distinguish between a *cis*- and a *trans*-constant.

The rate constants for water exchange in mononuclear ammine-aquachromium(III) complexes are ca. $0.6 \times 10^{-4} \text{ s}^{-1}$ with ammonia and ca. $0.1 \times 10^{-4} \text{ s}^{-1}$ with water in the *trans*-position relative to the reacting water ligand.⁹ The magnitudes of the rate constants, $k_{\text{md}(1-3)}$, for bridge formation, and their variation, indicates a mechanism with associative character in which intramolecular proximity between an attacking oxygen atom on one chromium atom and the other chromium atom is important for water release at the latter atom. The situation is illustrated in Fig. 3, which has similarities to structures proposed⁹ for water exchange in the above-mentioned mononuclear chromium(III) complexes. In the 4+ and 3+ charged monohydroxo-bridged dimers the existence of intramolecular $\text{H}-\text{O} \cdots \text{H} \cdots \text{O}-\text{H}$ hydrogen bonds favours this proximity and has the consequence, with the proposed model, that a *cis*- or *trans*-conformation with respect to a $\text{Cr}(\mu\text{-OH})(\mu\text{-H}_3\text{O}_2)\text{Cr}$ 'plane' will be retained as a *cis*- or *trans*-configuration, respectively, after bridge formation.

The higher rate constants for the 3+ relative to the 4+ charged dimers can now be explained by the presence of OH^- at position 1 in the former case, i.e. base catalysis. Furthermore, hydrogen bonding between oxygen atoms at positions 1 and 2 in the 3+ charged dimer may stabilize the *cis*-transition state relative to the *trans*-conformation, this being partly responsible for the observed difference between $k_{\text{mc}3}$ and $k_{\text{mt}3}$.

The reason for the small magnitude of $k_{\text{md}1}$ compared to $k_{\text{md}2}$ may be attributed to $\text{Cr}-\text{OH}$ being a better nucleophile than $\text{Cr}-\text{OH}_2$ in the suggested mechanism, with an essential degree of associative character. The magnitude of $k_{\text{md}1}$ is close to $k_{\text{md}1}$ for the aqua system and somewhat bigger than the rate of water exchange in mononuclear ammineaquachromium(III) complexes. It is striking, however, that $k_{\text{md}1}$ for the tetraammine system is ca. 50 times smaller. The reason for this is not obvious, but part of the enhanced rates in the systems with more

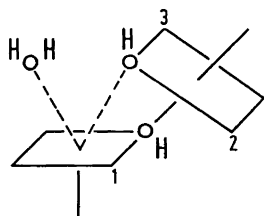


Fig. 3. The idealized transition-state structure proposed for the bridge formation/cleavage in the 3+ and 4+ charged species ($\text{O} = \text{oxygen atom}$). With the two remaining oxygen atoms placed in positions 1 and 2 the result is a *cis*-configuration, while it leads to a *trans*-configuration if they are placed in positions 1 and 3.

than one water ligand per chromium atom in a *cis*-position to the bridge may originate from additional, stabilizing, intramolecular $\text{H}_2\text{O} \cdots \text{H}-\text{O}-\text{H}$ hydrogen bonds between water ligands at the two chromium centers during the course of the reaction.

As mentioned in the introduction a salt of the trihydroxo-bridged dimer, $[(\text{NH}_3)_3\text{Cr}(\text{OH})_3\text{Cr}(\text{NH}_3)_3]^{3+}$, is also available.¹⁰ This dimer is unstable in aqueous solution, where it reacts rapidly to the dihydroxo-bridged *cis*-dimer, and it has actually been the source of the latter compound in the present investigation.¹ A forthcoming paper will deal with the $[\text{H}^+]$ and temperature influence on the rate of this irreversible bridge cleavage.¹¹

Experimental

Chemicals, dihydroxo-bridged compounds, apparatus and experimental conditions for the determination of the observed rate constants are identical to those described elsewhere.¹ The kinetic experiments were performed at 25.0°C with $10^{-7} < [\text{H}^+] < 1 \text{ M}$ in 1.0 M $(\text{Na,H})\text{ClO}_4$ and, for comparison, some in 4.0 M $(\text{Li,H})\text{ClO}_4$. $[(\text{H}_2\text{O})_2(\text{NH}_3)_3\text{Cr}(\text{OH})\text{Cr}(\text{NH}_3)_3(\text{H}_2\text{O})_2](\text{CF}_3\text{SO}_3)_{3.7}(\text{ClO}_4)_{1.3} \cdot 1.5\text{H}_2\text{O}^2$ was used as the monohydroxo-bridged reactant. The following section will deal with eqns. (1)–(3) and show a selected course of reaction.

Eqn. (1). This equation is analogous to that of the *cis*-*trans* isomerization.¹ The parameters in the least-squares refinement (with omission of the insignificant $[\text{H}^+]^2 K_{\text{d}0}^{-1}$ term) were $k_{\text{md}1}$, $k_{\text{md}2}$, $k_{\text{md}3}$, $K_{\text{m}1}$ and $K_{\text{m}2}$, while values of $K_{\text{m}1}/K_1 = 10^{-0.10} \text{ M}$ and of $K_{\text{d}1} = 10^{-5.11} \text{ M}$ were inserted as obtained in a different and more accurate way from experiments described elsewhere.^{1,2} The result of the refinement is given in Table 1 and Fig. 1.

Eqn. (2). For the uniexponential absorbance (A) vs. time (t) curves eqn. (2a) was used, and for biexponential ones

$$A(t)_{\text{obs}} = (A_0 - A_\infty)e^{-k_{\text{obs}}t} + A_\infty + \alpha t \quad (2a)$$

eqn. (2) was used in least-squares calculations of the observed rate constants k_{obs} , k_{md} and k_{d} . The last term, αt , in these expressions makes allowance for a small linear correction due to the loss of ammonia at $[\text{H}^+] < \text{ca. } 10^{-5} \text{ M}$. At 7 half-lives αt was at most 2–3% of $A_0 - A_\infty$, and at a given wavelength α was roughly proportional to the chromium concentration. Some of the added buffers exhibited absorbance below ca. 450 nm, but by choosing fixed wavelengths between 500 and 650 nm this was not a problem. Under these circumstances good fits to eqns. (2) and (2a) were obtained.

With reference to Scheme 2a, eqn. (2) can be elucidated as follows:

$$\partial[\text{m}]/\partial t = -(k_{\text{mt}} + k_{\text{mc}})[\text{m}]$$

$$\partial[\text{trans-d}]/\partial t = k_{\text{mt}}[\text{m}] + k_{\text{ct}}[\text{cis-d}] - k_{\text{tc}}[\text{trans-d}]$$

$$\partial[\text{cis-d}]/\partial t = k_{\text{mc}}[\text{m}] + k_{\text{tc}}[\text{trans-d}] - k_{\text{ct}}[\text{cis-d}]$$

With $k_{md} = k_{mt} + k_{mc}$, $k_d = k_{tc} + k_{ct}$ and $[m]_0$ being the initial monohydroxo-bridged dimer concentration these three differential equations are solved as¹²

$$[m] = [m]_0 e^{-k_{md}t}$$

$$[trans-d] = [m]_0 \left[\frac{k_{mt} - k_{ct}}{k_d - k_{md}} e^{-k_{md}t} - \left(\frac{k_{ct}}{k_d} + \frac{k_{mt} - k_{ct}}{k_d - k_{md}} \right) \times e^{-k_d t} + \frac{k_{ct}}{k_d} \right]$$

$$[cis-d] = [m]_0 \left[\frac{k_{mc} - k_{tc}}{k_d - k_{md}} e^{-k_{md}t} - \left(\frac{k_{ct}}{k_d} + \frac{k_{mc} - k_{tc}}{k_d - k_{md}} \right) \times e^{-k_d t} + \frac{k_{tc}}{k_d} \right]$$

With ϵ_m , ϵ_t and ϵ_c being the molar absorptivities of m,

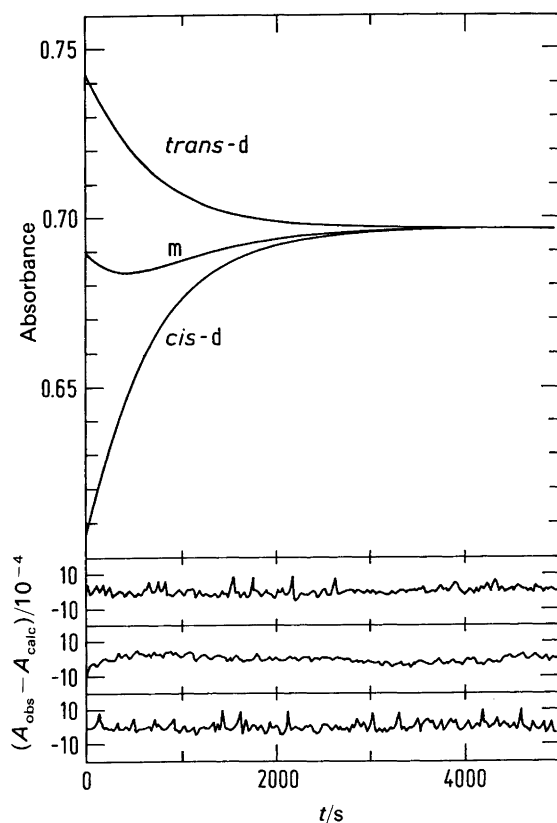


Fig. 4. An example of three spectrophotometric time (t) drives at 560 nm with $-\log [H^+] = 4.90$ and $C_{Cr} = 12.8$ mM (25.0°C, 1.0 M NaClO₄). The experiments represented by the upper and lower curves started with the dihydroxo-bridged *trans*- and *cis*-isomer, respectively, while the middle one started with the monohydroxo-bridged complex, all proceeding to the same equilibrium situation. The data treatment is explained in the text, and the result is given in Table 2. The A vs. t curves are the calculated ones, while the deviation from the experiments ($A_{obs} - A_{calc}$) is shown in the same sequence underneath.

trans-d and *cis*-d, respectively, the absorption, $A(t)$, at a given wavelength as a function of time is

$$A(t) = [m]_0 \left(\epsilon_m + \epsilon_t \frac{k_{mt} - k_{ct}}{k_d - k_{md}} + \epsilon_c \frac{k_{mc} - k_{tc}}{k_d - k_{md}} \right) e^{-k_{md}t} - [m]_0 \left[\epsilon_t \left(\frac{k_{ct}}{k_d} + \frac{k_{mt} - k_{ct}}{k_d - k_{md}} \right) + \epsilon_c \left(\frac{k_{tc}}{k_d} + \frac{k_{mc} - k_{tc}}{k_d - k_{md}} \right) \right] e^{-k_d t} + [m]_0 \left(\epsilon_t \frac{k_{ct}}{k_d} + \epsilon_c \frac{k_{tc}}{k_d} \right) = A_1 e^{-k_d t} + A_2 e^{-k_{md}t} + A_3$$

which, with $A_2 = A_0 - A_\infty - A_1$, $A_3 = A_\infty$ and addition of the at term, leads to eqn. (2).

Eqn. (3). From the previous section it follows that the expressions for A_1 , A_2 and A_3 are

$$A_1 = -[m]_0 \left[\epsilon_t \left(\frac{k_{ct}}{k_d} + \frac{k_{mt} - k_{ct}}{k_d - k_{md}} \right) + \epsilon_c \left(\frac{k_{tc}}{k_d} + \frac{k_{mc} - k_{tc}}{k_d - k_{md}} \right) \right]$$

$$A_2 = [m]_0 \left(\epsilon_m + \epsilon_t \frac{k_{mt} - k_{ct}}{k_d - k_{md}} + \epsilon_c \frac{k_{mc} - k_{tc}}{k_d - k_{md}} \right)$$

$$A_3 = [m]_0 \left(\epsilon_t \frac{k_{ct}}{k_d} + \epsilon_c \frac{k_{tc}}{k_d} \right) \quad (3a)$$

$$(A_1 + A_2 + A_3 = [m]_0 \epsilon_m = A_0)$$

From

$$A_1 + A_3 = [m]_0 \left(\epsilon_t \frac{k_{mt} - k_{ct}}{k_{md} - k_d} + \epsilon_c \frac{k_{mc} - k_{tc}}{k_{md} - k_d} \right) = \frac{[m]_0}{k_{md} - k_d} [(\epsilon_c - \epsilon_t)k_{mc} + \epsilon_t k_{md} - (\epsilon_t k_{ct} + \epsilon_c k_{tc})]$$

Table 2. An example of absorbance and rate constants obtained by use of eqn. (2) on the data shown in Fig. 4 (middle curve). The difference between the two models, I and II, is that model II uses the values of k_{md} and k_d unrefined as calculated separately from other experiments [Table 1, eqn. (1) and Ref. 1].

	I (5 parameters)	II (3 parameters)
A_0	0.6908	0.6898
A_∞	0.6963	0.6966
A_1	-0.047	-0.081
$k_{md}/10^{-4} \text{ s}^{-1}$	27	20.8 (not refined)
$k_d/10^{-4} \text{ s}^{-1}$	14	14.6 (not refined)
α/s^{-1}	0 (not refined)	0 (not refined)

using that $k_{mt} = k_{md} - k_{mc}$. With $\varepsilon_t k_{ct} + \varepsilon_c k_{tc} = A_3 k_d / [m]_0$ [eqn. (3a)] it then follows that

$$k_{mc} = \left[\frac{(A_1 + A_3)(k_{md} - k_d)}{[m]_0} + \frac{A_3 k_d}{[m]_0} - \varepsilon_t k_{md} \right] (\varepsilon_c - \varepsilon_t)^{-1}$$

$$= \frac{k_{md}(A_1 + A_3 - [m]_0 \varepsilon_t) - k_d A_1}{[m]_0 (\varepsilon_c - \varepsilon_t)}$$

leading to eqn. (3).

An example of an experiment for the determination of k_{mc} is shown in Fig. 4, and the result of least squares refinement of the middle curve data to eqn. (2) is given in Table 2. $[m]_0 \varepsilon_c$ and $[m]_0 \varepsilon_t$ were determined as 0.6052 and 0.7429, respectively, from the lower and upper curve data (Fig. 4) using eqn. (2a). Insertion of these values and those of column II of Table 2 into eqn. (3) gives $k_{mc} = 10.6 \times 10^{-4} \text{ s}^{-1}$ ($11.1 \times 10^{-4} \text{ s}^{-1}$ at 570 nm). The values of k_{mc} obtained from column I of Table 2 ($14 \times 10^{-4} \text{ s}^{-1}$ in this case) are considered more uncertain owing to the strong correlation between A_1 , k_{md} and k_d .

Acknowledgments. We thank Drs. Ole Mønsted and Johan Springborg for valuable help and discussions, and the Danish Natural Science Research Council for grants nos. 11-5962 and 11-6784 towards the purchase of the UV/VIS spectrophotometer and for the support of A.D., respectively.

References

1. Andersen, P. and Døssing, A. *Acta Chem. Scand.* 46 (1992) 354.
2. Andersen, P., Døssing, A. and Nielsen, K. M. *Acta Chem. Scand., Ser. A* 40 (1986) 142.
3. Springborg, J. In: Sykes, A. G., Ed., *Advances in Inorganic Chemistry*, Academic Press, New York 1988, Vol. 32, p. 55 and references therein.
4. Andersen, P., Døssing, A., Glerup, J. and Rude, M. *Acta Chem. Scand.* 44 (1990) 346.
5. Galsbøl, F., Larsen, S., Rasmussen, B. and Springborg, J. *Inorg. Chem.* 25 (1986) 290.
6. Chaudhuri, P., Nuber, B., Weiss, J. and Wieghardt, K. *Inorg. Chem.* 21 (1982) 3086.
7. Josephsen, J. and Schäffer, C. E. *Acta Chem. Scand.* 24 (1970) 2929.
8. Schwarzenbach, G. and Magyar, B. *Helv. Chim. Acta* 45 (1962) 1425.
9. Mønsted, L. and Mønsted, O. In: *Coordination Chemistry Reviews*, Elsevier, Amsterdam 1989, Vol. 94, p. 109 and references therein.
10. Andersen, P., Døssing, A., Larsen, S. and Pedersen, E. *Acta Chem. Scand., Ser. A* 41 (1987) 381.
11. Andersen, P. and Døssing, A. *Acta Chem. Scand.* 47 (1993) 24.
12. Alberty, R. A. and Miller, W. G. *J. Chem. Phys.* 26 (1957) 1231.
13. Marty, W. and Spiccia, L. *Polyhedron* 10 (1991) 619.
14. Grace, M. R. and Spiccia, L. *Polyhedron* 10 (1991) 2389.

Received April 10, 1992.